Magneto-optical and optical properties of Fe-rich Au-Fe alloy films near the fcc-bcc structural transformation region

Y. P. Lee
Quantum Photonic Science Research Center and Department of Physics, Hanyang University, 17 Haengdang-Dong, Sungdong-Ku, Seoul 133-791, Republic of Korea

Y. V. Kudryavtsev and V. V. Nemoshkalenko
Institute of Metal Physics, National Academy of Sciences of Ukraine, 36 Vernadsky strasse, 03142, Kiev-142, Ukraine

R. Gontarz
Institute of Molecular Physics, Polish Academy of Sciences, Smoluchowskiego 17, Poznań 60-179, Poland

J. Y. Rhee
Department of Physics, Hoseo University, Asan, Choongnam 336-795, Republic of Korea
(Received 9 April 2002; revised manuscript received 25 November 2002; published 25 March 2003)

A set of $Au_{1-x}Fe_x$ alloy films with $0<x<1$ have been prepared by rf sputtering onto glass substrates kept at 293 K. The x-ray diffraction study reveals fcc structures for the $Au_{1-x}Fe_x$ alloy films with $x<0.8$, and bcc structures for $x>0.80$. The equatorial-Kerr-effect (EKE) spectra for the $Au_{1-x}Fe_x$ alloy films with bcc and fcc types of structure show noticeably different spectral shapes and magnitudes from each other. Moreover, the EKE value in the UV region for the Fe-rich $Au_{1-x}Fe_x$ alloy films exceeds that for the pure Fe film. The observed blueshift and redshift of the low- and high-energy peaks, respectively, of the Fe-rich $Au_{1-x}Fe_x$ alloy films with respect to pure Fe are caused by differences in the optical constants between alloy and Fe films, which cannot explain, on the other hand, the enhancement of EKE value for the bcc $Au_{1-x}Fe_x$ alloys. The optical-conductivity (OC) spectra for the $Au_{1-x}Fe_x$ alloy films with bcc type of structure are characterized by an intense interband absorption peak at 2.0 eV, which is completely absent in the OC spectra of the $Au_{1-x}Fe_x$ alloy films with fcc type of structure. The spectra of absorptive part of the off-diagonal components of dielectric function for the investigated $Au_{1-x}Fe_x$ alloy and Fe films exhibit a double-peak structure; a peak near 1.8 eV (which does not depend on the composition or the structural state of alloy) and a high-energy peak. The latter is located at 3.3 eV for the $Au_{1-x}Fe_x$ alloy films with fcc type of structure and at 4.0–4.2 eV for the alloys with bcc structure as well as for the Fe film.

DOI: 10.1103/PhysRevB.67.104424 PACS number(s): 78.20.Ls, 78.66.Bz, 74.25.Ha

I. INTRODUCTION

Past-decade investigations on novel physical properties of metallic multilayered films (MLF), such as strong surface magnetic anisotropy, enhanced magneto-optical (MO) effect, quantum-confinement effect, and giant magnetoresistence, attract significant attention because of the fundamental interests and the practical applications. Au/Fe MLF system is one of them. The MO properties of Au/Fe layered structure have been intensively investigated experimentally[1–13] and theoretically,[13,14] however, some aspects are still unclear. Suzuki *et al.* discovered new peaks in the UV region of the MO spectra for Au/Fe layered structures, which are not related to bulk Fe, and explained this by the formation of quantum-well states in the ultrathin Fe sublayers grown on the Au substrate.[9–12] On the other hand, a lot of theoretical calculations reveal that the magnetic moment of the Fe sublayers in Au/Fe MLF is enhanced from $2.2\mu_B$ up to about $3\mu_B$ (depending on the structure or the geometry).[15–18] Furthermore, a small but oscillating (with the Au sublayer thickness) magnetic moment of the Au atoms is also well established.[15–18] It is well known that, fundamentally, the MO Kerr effect is caused by the simultaneous occurrence of spin polarization and spin-orbit coupling in a magnetic solid. Therefore, the enhancement of Kerr rotation in the UV region of spectra (or appearance of new peaks) of Au/Fe MLF can also be caused by either an increased magnetic moment at the Fe sites, a stronger spin-orbit coupling in the Au atoms, or an induced magnetic moment of the Au atoms.

It is natural to assume that the fabrication of Au/Fe MLF is accompanied by the spontaneous formation of alloylike regions near the interfaces between sublayers of the pure elements, which can, in turn, affect the physical properties of MLF. Indeed, Gavrilenko and Wu,[14] and also Uba *et al.*[13] mentioned that the agreement between experimental and calculated MO properties of Au/Fe MLF is significantly improved if the formation of alloylike regions is taken into account in the model.

Furthermore, an enhanced magnetic moment at the Fe sites up to $3\mu_B$ as well as an induced small magnetic moment at the Au sites in Au-Fe alloys were also observed experimentally[19] and forecasted theoretically.[20] However, later Guire *et al.* reported that $Au_{1-x}Fe_x$ alloys exhibit a constant Fe magnetic moment of $2.2\mu_B$ for $0.26<x<0.92$.[21]

Therefore, in order to understand the MO properties of Au/Fe MLF the MO properties of Au-Fe alloys (as one of the probable constituents in Au/Fe MLF) in a wide compositional range should also be known. The MO properties of a

TABLE I. Parameters of prepared and investigated Au-Fe alloy films.

Sample no.	Alloy composition	Film thickness (nm)	Sample no.	Alloy composition	Film thickness (nm)
I-1	$Fe_{0.008}Au_{0.992}$	482.4	II-1	$Fe_{0.015}Au_{0.985}$	188.2
I-2	$Fe_{0.018}Au_{0.982}$	417.9	II-2	$Fe_{0.011}Au_{0.989}$	251.0
I-3	$Fe_{0.023}Au_{0.977}$	354.8	II-3	$Fe_{0.035}Au_{0.965}$	224.1
I-4	$Fe_{0.034}Au_{0.966}$	227.9	II-4	$Fe_{0.038}Au_{0.962}$	231.4
I-5	$Fe_{0.053}Au_{0.947}$	153.0	II-5	$Fe_{0.074}Au_{0.926}$	148.0
I-6	$Fe_{0.118}Au_{0.882}$	119.7	II-6	$Fe_{0.160}Au_{0.840}$	92.3
I-7	$Fe_{0.270}Au_{0.730}$	94.9	II-7	$Fe_{0.314}Au_{0.686}$	95.3
I-8	$Fe_{0.436}Au_{0.564}$	86.7	II-8	$Fe_{0.590}Au_{0.410}$	102.2
I-9	$Fe_{0.690}Au_{0.310}$	95.7	II-9	$Fe_{0.771}Au_{0.229}$	118.1
I-10	$Fe_{0.799}Au_{0.201}$		II-10	$Fe_{0.863}Au_{0.137}$	180.3
I-11	$Fe_{0.908}Au_{0.092}$	152.1	II-11	$Fe_{0.926}Au_{0.074}$	228.9
I-12			II-12	$Fe_{0.978}Au_{0.022}$	287.2

medium {i.e., the off-diagonal components of its dielectric function, DF $(\tilde{\varepsilon})$ $[\tilde{\varepsilon}_{xy}=-\tilde{\varepsilon}_{yx}=i\tilde{\varepsilon}';\tilde{\varepsilon}'=\varepsilon_1'-i\varepsilon_2']\}$ cannot be determined without knowing its optical properties [i.e., the diagonal components of the DF $(\tilde{\varepsilon}_{xx}=\tilde{\varepsilon}_{yy}=\tilde{\varepsilon}_{zz}=\varepsilon=\varepsilon_1-i\varepsilon_2$, $\varepsilon_1=n^2-k^2$, and $\varepsilon_2=2nk$, where n and k are index of refraction and coefficient of extinction, respectively). As far as we know, the MO and optical properties of Au-Fe alloy films have not been investigated yet at all.

Thus, the purpose of this work is to prepare Fe-Au alloy films and to investigate their MO and optical properties. This paper has the following structure. In Sec. II, we describe the experimental details. Section III is devoted to a study of the structural and the optical properties of Au-Fe alloy films. In Sec. IV, the experimental MO properties of Au-Fe alloy films are presented and discussed.

II. EXPERIMENTAL PROCEDURE

Two sets of $Au_{1-x}Fe_x$ alloy films with $0<x<1$ have been prepared by the simultaneous rf sputtering of Au and Fe targets onto large glass substrates (25×120 mm^2 in size), which were positioned in parallel to a ''line'' connecting the Au and Fe targets and were kept at room temperature (RT). The relative position of the substrate with respect to the Au and Fe targets was slightly changed in the second deposition for the alloy film. Therefore, the alloy compositions of both films are slightly different. After the deposition, both films were cut into 12 pieces along the short side of substrate, and 2×12 alloy samples were obtained. The composition of each Au-Fe alloy sample was determined at its central part by x-ray fluorescence. The parameters of the prepared $Au_{1-x}Fe_x$ alloy films are shown in Table I. Pure Fe and Au films of about 200 nm in thickness were also prepared at the same deposition conditions. The structural characterization of $Au_{1-x}Fe_x$ alloy films was performed by using high-angle x-ray diffraction (XRD) with Co-K_α radiation. The magnetic properties [in-plane magnetization loops, $M(H)$] were measured at RT and in a magnetic field of 1.5 T with a vibrating sample magnetometer (VSM).

The MO equatorial Kerr effect (EKE) of $Au_{1-x}Fe_x$ alloy films was investigated at RT by the dynamical method[22] using the *p*-plane polarized light at angles of incidence of 66° and 75° in a spectral range of 248–1130 nm (5.0–1.1 eV), and in an ac magnetic field of 950 Oe (a maximum ac magnetic field available to us). The EKE value, $\delta_p=\Delta I/I_o$, is the relative change in intensity of the reflected light caused by the magnetization of a sample in an external magnetic field whose direction is transverse to the plane of light incidence. The absorptive ε_2' and the dispersive ε_1' parts of the off-diagonal components of the DF were determined for several $Au_{1-x}Fe_x$ alloy films (nearly equiatomic and $Au_{0.25}Fe_{0.75}$ compositions) by using the corresponding experimental results obtained in the optical and the MO studies. The optical properties were measured by the polarimetric Beattie technique[23] at RT in a spectral range of 235–2500 nm (5.3–0.5 eV) at a fixed incidence angle of 73°.

We focus our MO study on the Fe-rich $Au_{1-x}Fe_x$ alloy films. Therefore, in order to secure more systematic change in alloy composition for the study we chose various samples from both sets of films.

III. STRUCTURAL AND OPTICAL STUDIES

The high-angle XRD patterns for the second set of $Au_{1-x}Fe_x$ alloy films, together with that for the pure Fe film, are shown in Fig. 1. All the XRD spectra exhibit only one diffraction peak. The location and the width (see inset in Fig. 1) of this diffraction peak depend remarkably on sample number (the alloy composition). The compositional dependence of the interplanar spacing d, calculated from the peak position, reveals a nearly linear decrease from the value of (111) spacing for bulk Au (an fcc type of structure) by increasing the Fe content from $x\approx0$ up to $x\approx0.75$–0.80 (see Fig. 2). At $x\approx0.80$, the interplanar spacing abruptly decreases and then keeps decreasing with the Fe content towards the value of (110) spacing for bulk Fe (a bcc type of structure) at nearly the same rate as for the $0<x\leqslant0.80$ range. It is known that at RT, Au has a very limited solubility in Fe and vice versa, however, at high (about 1200 K) temperatures, the region with an equilibrium terminal solid so-

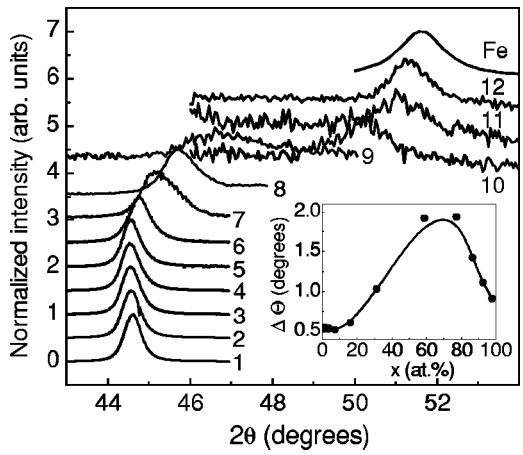

FIG. 1. Normalized XRD spectra, taken with Co K_α radiation, for the second set of $Au_{1-x}Fe_x$ alloy films (see Table I) and an Fe film. Inset shows the dependence of the diffraction linewidth on the Fe content.

lution based on fcc Au is stretched up to around a composition of $Au_{0.30}Fe_{0.70}$.[24] The compositional dependence of lattice parameter [(111) interplanar spacing] for this equilibrium at 1200 K of alloy with $x \leqslant 0.65$ shows a rather similar behavior to the experimentally observed one for Au-Fe alloy films (see Fig. 2).[25] However, it is seen that the deviation between these two curves increases with x, probably indicating an accumulation of strain in the films with increasing the Fe content. At $x \approx 0.80$, this strain causes the structural transformation of lattice to the bcc type of structure. It can be concluded that the experimentally observed $d(x)$ dependence reflects a structural fcc-bcc transformation in $Au_{1-x}Fe_x$ alloy, which takes place at $x \approx 0.80$. This fact is consistent with the results by Guire *et al.*, except that their critical concentration for the structural transformation of $x \approx 0.75$.[21] A noticeable increase of the diffraction linewidth in the transitional region indicates the adaptation process of crystalline structure of the alloy to new quasi-equilibrium conditions. Thus, it seems to us that the deposition onto a substrate at RT can be considered as a sort of quenching which retains the high-temperature equilibrium down even at RT.

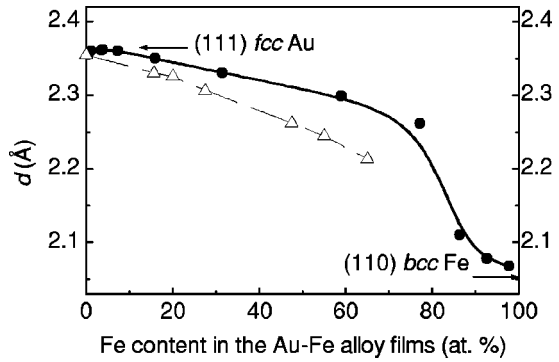

FIG. 2. Fe-content dependence of the interplanar spacing d for the investigated $Au_{1-x}Fe_x$ alloy films (solid circles). Line is a guide for the eyes. Open triangles show the compositional dependence of d for the equillibrium bulk Au-Fe alloys at $T = 1200$ K (Ref. 25).

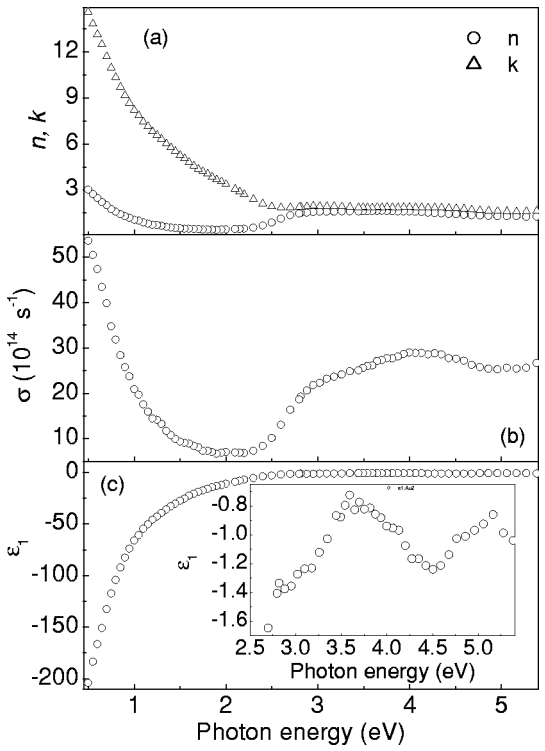

FIG. 3. Experimental optical properties of a Au film. Inset in (c) shows an expanded view of the ε_1 spectrum.

The optical properties [n, k, ε_1 and optical conductivity (OC; $\sigma = \varepsilon_2 \omega / 4\pi$)] of pure Au and Fe films are shown in Figs. 3 and 4, respectively. The purpose is to show the boundaries between which the optical properties of $Au_{1-x}Fe_x$ alloy films might be observed. The optical properties of Au have been well studied experimentally and explained theoretically.[26–32] Our experimental data for Au film reproduce nicely all the basic features of the OC spectrum of Au, namely, a sharp threshold in the 2.5-eV range, associated with the beginning of interband transitions between the fifth and the sixth band, a feature at 4 eV caused by an electron excitation from the fifth to the seventh band near the L-symmetry point, and an intense intraband absorption below $\hbar\omega \approx 2$ eV. The strong intraband absorption is also manifested by a very large and negative value of ε_1 at $\hbar\omega < 2$ eV.

The optical properties of Fe film (see Fig. 4) are also in a great agreement with the experimental[33,34] and theoretical[35–39] literature data exhibiting a strong interband absorption peak near 2.4 eV. This peak is known to be produced by electron excitations mainly in the minority-spin sub-bands which are located in the column of an irregular cross section rising normally from near the center of Γ-H-N plane in the irreducible wedge of the Brillouin zone.[35,36,38]

The optical properties of the investigated $Au_{1-x}Fe_x$ alloy films are presented in Fig. 5, together with those of Au and Fe films for the comparison. In general, the σ and ε_1 spectra of the alloys do not exhibit any new feature that is not typical for Fe or Au. However, the transition from pure Fe to the Fe-rich bcc $Au_{1-x}Fe_x$ alloys leads to an expected redshift of the main absorption peak in the OC spectra [see Fig. 5(c)].

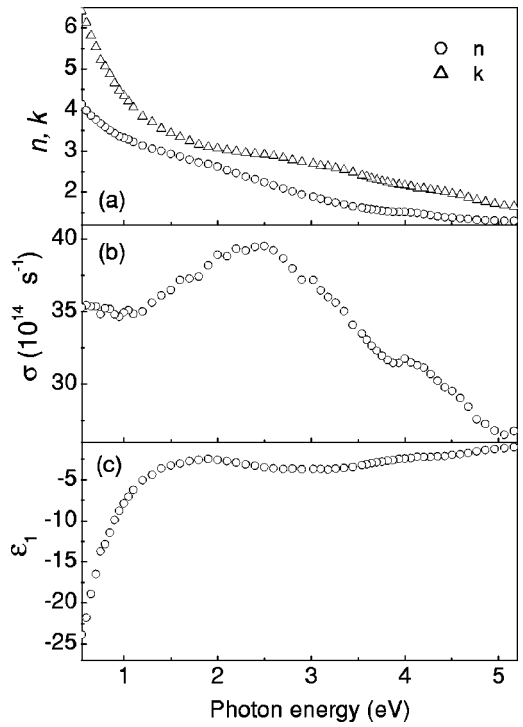

FIG. 4. Experimental optical properties of an Fe film. (a) presents the spectra of n and k, (b) shows the OC spectrum, and (c) presents the real part of the diagonal components of DF.

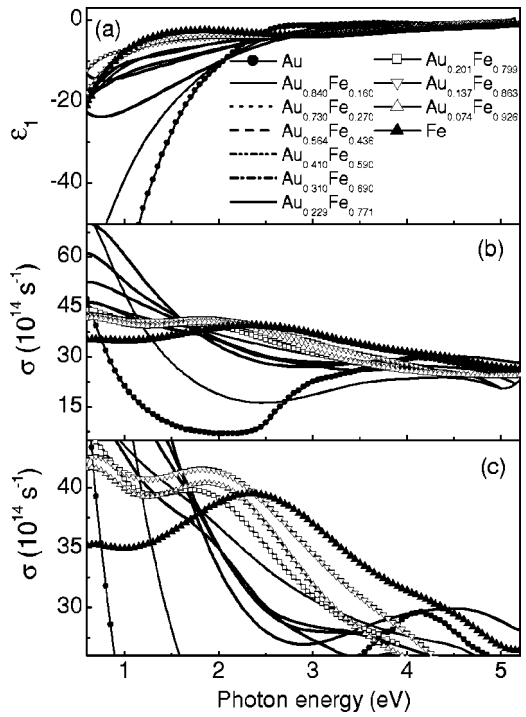

FIG. 5. Fitted ε_1 (a) and σ (b,c) spectra for the investigated $Au_{1-x}Fe_x$ alloy as well as Fe and Au films. (c) shows an expanded view of (b).

Indeed, the Fe-rich $Au_{1-x}Fe_x$ alloy films with the bcc type of structure have a larger lattice parameter than that of pure Fe (see Fig. 2). This should induce a narrowing of the electron band structure towards the Fermi level. Therefore, the initial and the final states responsible for formation of this peak get closer to each other, which produces a shift of the peak to the low-energy side. Furthermore, a reduced number of the nearest-neighboring Fe atoms in the Fe-rich $Au_{1-x}Fe_x$ alloy films with respect to pure Fe also weakens the interaction between Fe atoms and hence narrows the width of $3d$-Fe band. A further decrease in the Fe content down to $x \approx 0.8$ leads to the bcc-fcc structural transformation in $Au_{1-x}Fe_x$ alloy films, which is accompanied by the complete disappearance of the peak. This radical change in the optical properties of $Au_{1-x}Fe_x$ alloy films is an evidence for significant changes in the electron energy structure caused by the structural transformation. On the other hand, a transition from Au to the Au-rich $Au_{1-x}Fe_x$ alloy with the fcc type of structure induces a gradual blurring of the Au interband-absorption edge with increasing x.

IV. MAGNETO-OPTICAL PROPERTIES

The MO properties of a sample should be measured in a saturated magnetic field. Therefore, the usual first step for the MO experiment is to check the magnetic-field dependence of MO response. The $\delta_p(H)$ dependences for the investigated $Au_{1-x}Fe_x$ alloy films are shown in Fig. 6. It is seen that the responses are changed significantly according to x, and that the presented curves can be classified into two groups bearing a soft ($Au_{1-x}Fe_x$ alloy films with the bcc type of structure) and a hard ($Au_{1-x}Fe_x$ alloy films with the fcc type of structure) magnetic behavior. The $\delta_p(H)/\delta_p(950)$ dependence for $Au_{0.229}Fe_{0.771}$ alloy film lies at the border between two groups, which suggests an intermediate structural state in the film. The in-plane saturation was not achieved for some of our samples. Hence, in order to compare with the other samples, direct $M(H)$ measurements by VSM were employed. In general, the $\delta_p(H)/\delta_p(950)$ dependence obtained from the MO measurements is in a good agreement with the $M(H)$ results. Therefore, in those cases where the saturation of MO response was not achieved at an ac magnetic field of 950 Oe, the experimental EKE spectra were artificially ''saturated'' by using the corresponding scal-

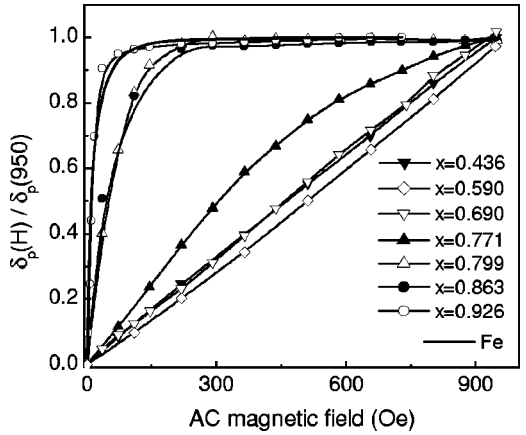

FIG. 6. An ac magnetic-field dependence of the MO response for the invetsigated $Au_{1-x}Fe_x$ alloy and Fe films.

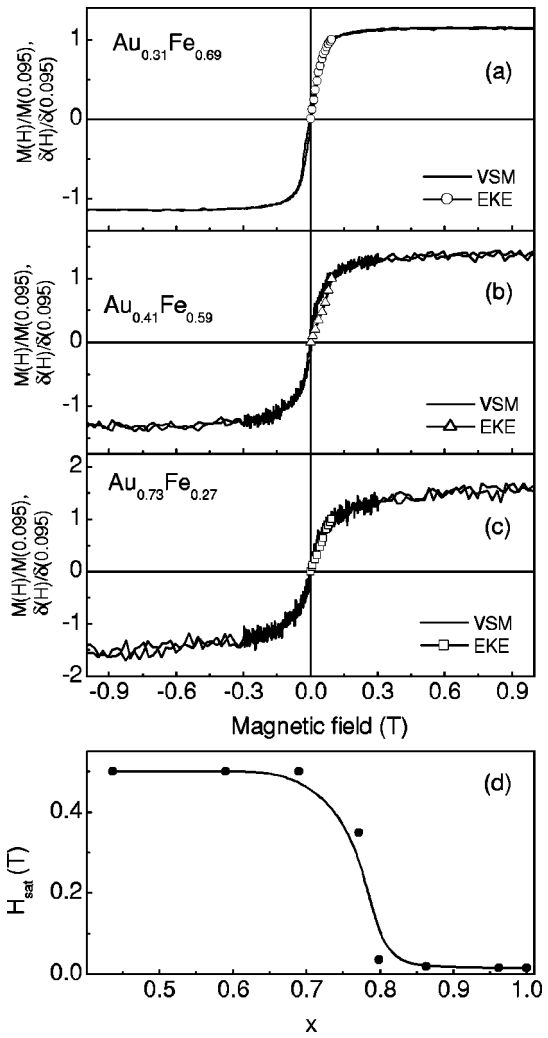

FIG. 7. Magnetic-field dependences of the magnetization and the MO response for the invetsigated $Au_{1-x}Fe_x$ alloy films with the fcc type of structure [(a)–(c)]. (d) shows the Fe-content dependence of the in-plane saturation magnetic field for the investigated $Au_{1-x}Fe_x$ alloy films.

ing factors determined from the comparison of the $M(H)$ and $\delta_p(H)$ curves, normalized with respect to the respective values at $H=0.095$ T (see Fig. 7). Figure 7(d) summarizes these results and shows the compositional dependence of the in-plane saturation magnetic field for the investigated $Au_{1-x}Fe_x$ alloy films. It is seen that at $x=0.8$, i.e., at the bcc-fcc structural transformation, the saturation field increases abruptly with decreasing x. Such a behavior can be explained, for example, by a noticeable perpendicular magnetic anisotropy formed in the $Au_{1-x}Fe_x$ alloy films with the fcc type of structure.

The experimental (and the artificially saturated) EKE spectra for the investigated $Au_{1-x}Fe_x$ alloy films, together with the EKE spectra for film and bulk Fe, are presented in Fig. 8. The EKE spectrum for Fe film reveals an intense peak at 1.7 eV, which has an excellent resemblance in shape and peak position to the literature data for bulk Fe,[40] however, its magnitude is smaller by about 25%. The structural dependence of the EKE for Fe film was specially examined by

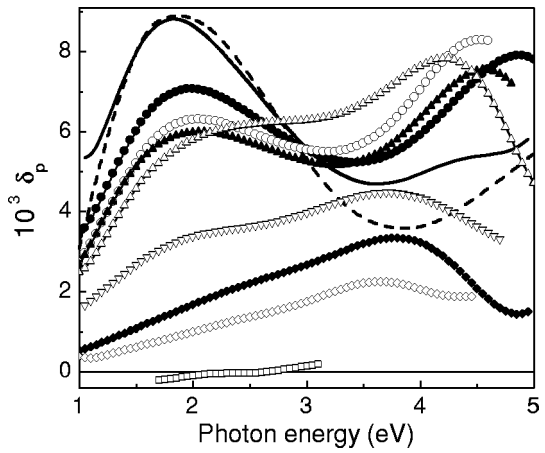

FIG. 8. EKE spectra measured at $\varphi=66°$ for pure Fe film (solid line), and $Au_{1-x}Fe_x$ alloy films with $x=0.926$ (solid circles), 0.863 (open circles), 0.799 (solid up-triangles), 0.771 (open up-triangles), 0.690 (open down-triangles), 0.590 (solid diamonds), 0.436 (open diamonds) and 0.270 (open squares). Dashed line shows the EKE spectrum for bulk Fe, measured at 70° and plotted with a scaling factor of 0.75 (Ref. 40).

Menéndez *et al.*[41] They show that the grain-size effect can influence significantly on the MO response. Therefore, the smaller EKE value of our Fe film might be relevant to a difference in the grain size between film and bulk Fe.

A transition from Fe to the Fe-rich $Au_{1-x}Fe_x$ alloy films with the bcc type of structure leads to a certain decrease of the MO response in the low-energy region and to a blue shift of the low-energy maximum by about 0.2 eV. On the other hand, the EKE value in the UV region is noticeably larger than that for pure Fe showing a high-energy peak (or the low-energy tail of a peak whose maximum is positioned beyond the investigated spectral range) of nearly the same intensity. It can be assumed that the high-energy peak has the same origin as a peak at 5.5–6.0 eV in the EKE spectrum for bulk Fe.[22] Contrary to the low-energy peak, this high-energy one exhibits a redshift with decreasing Fe content.

The EKE spectra for $Au_{1-x}Fe_x$ alloy films with the fcc type of structure have a substantially different spectral shape (the low-energy peak is nearly absent or very weak, but the high-energy peak continues to shift to the low-energy side) and significantly smaller values. The EKE spectrum for $Au_{0.73}Fe_{0.27}$ shows an extremely low intensity (if any). According to Guire *et al.*, the Curie temperature T_C for $Au_{1-x}Fe_x$ alloy films reaches RT at about $x\approx 0.20$,[21] which is close to our estimation for T_C based on these MO measurements.

Let us try to elucidate possible reasons for the EKE enhancement in the UV region of spectra observed for $Au_{1-x}Fe_x$ alloy films with the bcc type of structure. It is clear that in this case the confinement effect, as suggested by Suzuki and co-workers[9–12] for the explanation of new structures in the MO spectra of Fe/Au layered systems, has no place and should be excluded, first of all, from our consideration.

It is well known that the MO response like EKE is determined by both MO and optical parameters of a medium. The

transverse or equatorial Kerr effect observed at an angle of incidence φ can be expressed with the diagonal and off-diagonal components of DF as[42]

$$\delta_p = 2\sin 2\varphi\left(\frac{A\varepsilon_1'}{A^2+B^2}+\frac{B\varepsilon_2'}{A^2+B^2}\right), \tag{1}$$

where

$$A=\varepsilon_2(2\varepsilon_1\cos^2\varphi-1),$$

$$B=(\varepsilon_2^2-\varepsilon_1^2)\cos^2\varphi+\varepsilon_1-\sin^2\varphi.$$

Therefore, appearance of a new peak (or an enhancement of the MO response) in the UV region observed in the EKE spectra for $Au_{1-x}Fe_x$ alloy films may originate from changes in the optical parameters of alloy with respect to Fe. For a rough judgement for this possible reason, simulations of the EKE spectra for the Fe-rich $Au_{1-x}Fe_x$ alloy films have been carried out in the framework of effective-medium approximation (EMA). In this procedure, a nearly linear decrease in the magnetization of Au-Fe alloys with the decreasing Fe content was assumed.[21] We also assumed that the only source for the MO response from this alloy is the constituent Fe. First, the off-diagonal components of the DF for Fe film were calculated by using the measured EKE at two angles of incidence, the measured optical constants of Fe, and Eq. (1). The obtained spectra are coincident excellently with the published experimental[22] and theoretical[37–39] results. We considered two models. The off-diagonal components of the DF of $Au_{1-x}Fe_x$ alloy were chosen to be those of pure Fe, scaled by the Fe contents x, i.e., $\varepsilon'_{1,2(Au_{1-x}Fe_x)}=x\varepsilon'_{1,2(Fe)}$ (in model 1). In the second model, the enhancement of magnetic moment at the Fe sites, predicted by the theory,[20] for Au-Fe alloys with respect to pure Fe was also taken into account, i.e., $\varepsilon'_{1,2(Au_{1-x}Fe_x)}=E_F x\varepsilon'_{1,2(Fe)}$, where E_F is the enhancement factor. For both models, the measured ε_1 and ε_2 of the corresponding alloys were used as the diagonal components of DF. The results are shown in Fig. 9. It is seen that the simulated EKE spectra manifest two peaks shifted in comparison with those of Fe, but that the positions are coincident perfectly with the corresponding experimental ones. However, for both models the magnitudes of the simulated EKE spectra in the $\hbar\omega>3.5$ eV energy range are smaller than the experimentally observed ones. The EKE spectra, simulated for $Au_{1-x}Fe_x$ alloy with smaller x (not shown here), exhibit a worse correspondence with the experiment, probably because of inadequacy of such an approach for Au-Fe alloys far from the Fe-rich region. Thus, one can conclude that the blueshift and redshift (with respect to pure Fe) of the low- and high-energy peaks, respectively, in the EKE spectra for the Fe-rich $Au_{1-x}Fe_x$ alloy films result from differences in the optical constants between alloys and Fe, while this factor does not explain the enhancement of MO responses from the Fe-rich $Au_{1-x}Fe_x$ alloy films.

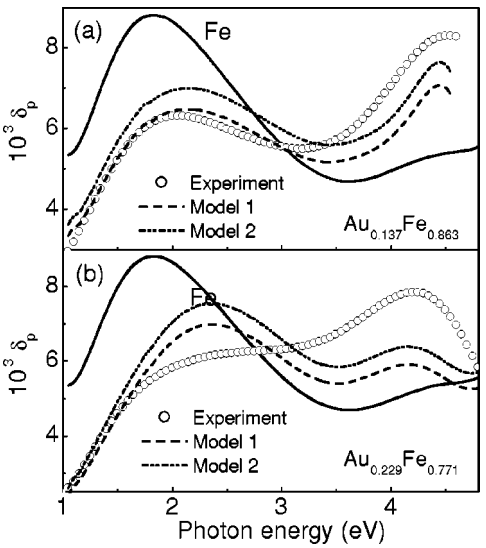

FIG. 9. Experimental and simulated EKE spectra for (a) $Au_{0.137}Fe_{0.863}$ and (b) $Au_{0.229}Fe_{0.771}$ alloy films shown together with the experimental EKE spectrum for pure Fe film.

In order to understand further the observed experimental results, the off-diagonal components of DF were calculated for Au-Fe alloys with the bcc and the fcc types of crystalline structure ($Au_{0.137}Fe_{0.863}$ and $Au_{0.41}Fe_{0.59}$, respectively) and in the intermediate region ($Au_{0.229}Fe_{0.771}$). For this purpose, additional EKE measurements at the second angle of incidence (75°) have been carried out. The calculated $\varepsilon_1'(\hbar\omega)^2$ and $\varepsilon_2'(\hbar\omega)^2$ spectra, together with the corresponding spectra for Fe film, are shown in Fig. 10. The validity of the obtained off-diagonal components for

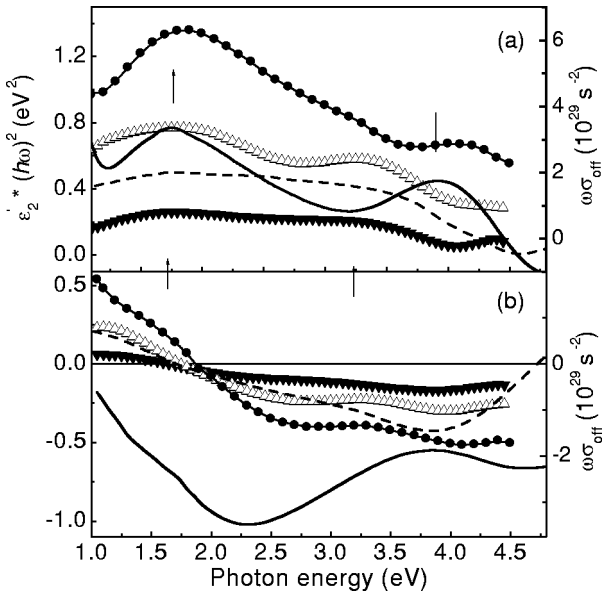

FIG. 10. Calculated spectra for (a) the absorptive and (b) the dispersive parts of the off-diagonal components of DF for $Au_{1-x}Fe_x$ alloy films with $x=0.59$ (solid down-triangles), 0.771 (open up-triangles) and 0.863 (solid circles). Solid and dashed lines present the corresponding spectra of Fe film and $(Au/Fe)_{20}$ MLF, respectively.

these alloys and Fe film was checked by calculating the EKE spectra using Eq. (1). The calculated EKE spectra perfectly reproduce the corresponding experimental EKE ones. In Fig. 10, we also include the literature data for $(Au/Fe)_{20}$ MLF which can be considered as an ordered $Au_{0.50}Fe_{0.50}$ alloy with an $L1_o$ type of structure.[13] All the spectra of absorptive part of the off-diagonal components for DF have a double-peak structure : a low-energy peak at 1.8 eV (which does not change the position by the fcc-bcc structural transformation), and a high-energy peak at about 3.3 eV for the fcc type of structure (or for the intermediate one) and at about 4 eV for the bcc type of structure (or for pure Fe film). Thus, the further redshift of the high-energy peak in the EKE spectra of $Au_{1-x}Fe_x$ alloys with decreasing x is induced additionally by changes in the $\varepsilon_2'(\hbar\omega)^2$ spectra of alloys.

It should be emphasized here that the magnitude of the $\varepsilon_2'(\hbar\omega)^2$ spectrum for $Au_{0.137}Fe_{0.863}$ alloy film is larger not only than that of the fcc or the intermediate alloy, but also that of pure Fe film. Such an enhancement cannot be explained with a more perfect structure in this range of x than the other because the structural superiority, if any, should be manifested more significantly in the optical properties (see Fig. 5). Furthermore, all the samples were prepared at the same deposition conditions.

To explain further the MO and the optical properties of Au-Fe alloys, we would like to refer to the previous first-principles calculations made for Fe-based MLF. The origin of an enhanced MO Kerr effect from ultrathin Fe- or Co-based multilayers was theoretically studied by Guo and Ebert.[43,44] It was shown that, for Fe/Pt MLF, a greatly stronger spin-orbit coupling in the heavy Pt atoms is the predominant microscopic factor. The magnetic moment of the Pt atoms is mainly due to a direct hybridization between the spin-integrated Pt orbitals and the spin-polarized Fe orbitals. In other words, through the direct orbital hybridization, a spin moment of the magnetic Fe atom is transferred to the nonmagnetic Pt atom and the strong spin-orbit coupling of the heavy Pt atoms, in turn, affects the Fe atoms. A similarity can be observed in a system comprising another heavy metal Au, i.e., in Au-Fe alloy system. Indeed, the first-principles calculations for $[\mathrm{Fe}(n\mathrm{ML})/\mathrm{Au}(n\mathrm{ML})]_N$ superlattices with $1 \leqslant n \leqslant 6$, where n is an integer number and ML denotes monolayer revealed that a structure near 4 eV is ascribed to an optical transition from the Au $5d$ state to the Au $5f$ hybridized with Fe $3d$ in the minority-spin band. By the detailed analysis of the band structure and the transition matrix elements, it was found that the structure around 4 eV in case of $n=1$ (equivalent to $Au_{0.50}Fe_{0.50}$ alloy) originates mainly from the $d\downarrow \rightarrow f\downarrow$ transition at the Au sites, in which the final state $f\downarrow$ is hybridized with the Fe $(3d\downarrow)$ state. In other words, this transition can be regarded as $Au(5d\downarrow) \rightarrow Fe(3d\downarrow)$.[8] The observed enhancement in the $\varepsilon_2'(\hbar\omega)^2$ spectra for $Au_{0.137}Fe_{0.863}$ alloy film, with respect to Fe or fcc $Au_{1-x}Fe_x$ alloys, results probably from a competition between this mechanism and an increase in the magnetization with increasing the Fe content. However, a more definite elucidation can be achieved by performing the first-principles calculations for the optical properties of these Au-Fe alloys, which are underway.

V. SUMMARY

The summary is given in the following points.

(1) A set of $Au_{1-x}Fe_x$ alloy films with $0<x<1$ have been prepared by rf sputtering onto glass substrates kept at RT. The XRD study revealed a fcc structure for $Au_{1-x}Fe_x$ alloy films with $x<0.8$, and a bcc structure for $x>0.80$.

(2) The EKE, OC, and ε_1 spectra for $Au_{1-x}Fe_x$ alloy films with the fcc and the bcc types of structure have been measured at RT.

(3) The EKE spectra for $Au_{1-x}Fe_x$ alloy films with the bcc and the fcc types of structure showed noticeably different spectral shapes and magnitudes. Moreover, the MO response for the Fe-rich $Au_{1-x}Fe_x$ alloy films exceeds that for pure Fe film.

(4) A simulation of the EKE spectra for the Fe-rich $Au_{1-x}Fe_x$ alloys, made in the framework of EMA, allowed us to conclude that the observed blueshift and redshift (with respect to pure Fe) of the low- and the high-energy peaks, respectively, in the EKE spectra of $Au_{1-x}Fe_x$ alloy films are caused by differences in the optical constants between alloy and Fe, while this cannot explain the enhancement of MO response in the UV region of spectra for the bcc $Au_{1-x}Fe_x$ alloys.

(5) The optical properties of all the investigated alloys lie between those of pure Fe and Au. The OC spectra for $Au_{1-x}Fe_x$ alloy films with the bcc type of structure are characterized by an interband absorption peak at 2.0 eV which has probably the same nature as an absorption peak at 2.4 eV of Fe. This peak is completely absent in the OC spectra of $Au_{1-x}Fe_x$ alloy films with the fcc type of structure.

(6) The off-diagonal components of DF for several $Au_{1-x}Fe_x$ alloy films and Fe film have been experimentally determined. The $\varepsilon_2'(\hbar\omega)^2$ spectra exhibit a double-peak structure: a peak near 1.8 eV (which does not depend on the composition or the structural state of alloy) and a high-energy peak. The latter is positioned at 3.3 eV for $Au_{1-x}Fe_x$ alloy films with the fcc type of structure and at about 4.0–4.2 eV for those with the bcc structure as well as for Fe film.

(7) The structural bcc-fcc transformation leads to an abrupt increase in the in-plane saturation magnetic field. This fact can be explained by the appearance of a perpendicular magnetic anisotropy in the fcc phase of alloy.

ACKNOWLEDGMENTS

This work was supported by the KOSEF through Quantum Photonic Science Research Center, by the MOST, Korea, and by Korea Research Foundation Grants (Grants Nos. KRF-2001-015-DS0015 and KRF-01-DP0193).

[1] T. Katayama, H. Awano, and Y. Nishihara, J. Phys. Soc. Jpn. **55**, 2539 (1986).
[2] Š. Višňovský, R. Lopušnik, M. Nývlt, A. Das, R. Krishnan, M. Tessier, Z. Frait, P. Aitchison, and J.N. Chapman, J. Magn. Magn. Mater. **198-199**, 480 (1999).
[3] R. Krishnan, M. Nývlt, and Š. Višňovský, J. Magn. Magn. Mater. **175**, 90 (1997).
[4] K. Takanashi, S. Mitani, H. Fujimori, K. Sato, and Y. Suzuki, J. Magn. Magn. Mater. **177-181**, 1199 (1998).
[5] K. Takanashi, S. Mitani, M. Sano, H. Fujimori, H. Nakajima, and A. Osawa, Appl. Phys. Lett. **67**, 1016 (1995).
[6] K. Takanashi, S. Mitani, K. Himi, and H. Fujimori, Appl. Phys. Lett. **72**, 737 (1998).
[7] K. Sato, A. Kodama, M. Miyamoto, K. Takanashi, H. Fujimori, and T. Rasing, J. Appl. Phys. **87**, 6785 (2000).
[8] K. Sato, E. Takeda, M. Akita, M. Yamaguchi, K. Takanashi, S. Mitani, H. Fujimori, and Y. Suzuki, J. Appl. Phys. **86**, 4985 (1999).
[9] Y. Suzuki, T. Katayama, S. Yoshida, K. Tanaka, and K. Sato, Phys. Rev. Lett. **68**, 3355 (1992).
[10] W. Geerts, Y. Suzuki, T. Katayama, K. Tanaka, K. Ando, and S. Yoshida, Phys. Rev. B **50**, 12 581 (1994).
[11] Y. Suzuki, T. Katayama, A. Thiaville, K. Sato, M. Taninaka, and S. Yoshida, J. Magn. Magn. Mater. **121**, 539 (1993).
[12] T. Katayama, Y. Suzuki, and W. Geerts, J. Magn. Magn. Mater. **158-162**, 5364 (1996).
[13] L. Uba, S. Uba, V.N. Antonov, A.N. Yaresko, T. Ślezak, and J. Korecki, Phys. Rev. B **62**, 13 731 (2000).
[14] V.I. Gavrilenko and R. Wu, J. Appl. Phys. **85**, 5112 (1999).
[15] J.M. MacLaren, M.E. McHenry, S. Crampin, and M.E. Eberhart, J. Appl. Phys. **67**, 5406 (1990).
[16] Z.P. Shi, J.F. Cookie, Z. Zhang, and B.M. Klein, Phys. Rev. B **54**, 3030 (1996).
[17] M. Ichimura and A. Sakuma, J. Magn. Magn. Mater. **177-181**, 1311 (1998).
[18] J.T. Wang, Z.Q. Li, Q. Sun, and Y. Kawazoe, J. Magn. Magn. Mater. **183**, 42 (1998).
[19] W. Felsch, Z. Angew. Phys. **29**, 217 (1970).
[20] B. Sanyal, P. Biswas, T. Saha-Dasgupta, A. Mookerjee, Ain-ul Huda, N. Choudhury, M. Ahmed, and A. Halder, J. Phys.: Condens. Matter **11**, 1833 (1999).
[21] T.R. Guire, J.A. Aboaf, and E. Klokholm, J. Appl. Phys. **52**, 2205 (1981).
[22] G.S. Krinchik and V.A. Artemév, Zh. Eksp. Teor. Fiz. **53**, 1901 (1967) [Sov. Phys. JETP **26**, 1080 (1968)].
[23] J.R. Beattie and G.M. Conn, Philos. Mag. **46**, 235 (1955).
[24] *Binary Alloy Phase Diagrams*, edited by T.B. Massalski (American Society for Metals, Metals Park, OH, 1986), Vol. I, p. 1100.
[25] O.M. Barabash and Y.N. Koval, *Crystalline Structure of Metals and Alloys* (Naukova Dumka, Kiev, 1986), pp. 324–325.
[26] V.G. Padalka and I.N. Shklyarevskij, Opt. Spectrosc. **11**, 527 (1961).
[27] G.P. Motulevich and A.A. Shubin, J. Exp. Theor. Phys. **47**, 840 (1964).
[28] P.G. Pells and M. Shiga, J. Phys. C **2**, 1835 (1969).
[29] P. Winsemius, H.P. Lengkeek, and F.F. van Kampen, Physica B & C **79**, 529 (1975).
[30] J.H. Weaver, C. Krafka, D.W. Lynch, and E.E. Koch, *Optical Properties of Metals in Physical Data* (Fachinformationszentrum, Karlsruhe, 1981).
[31] N.E. Christiansen and B.O. Seraphin, Phys. Rev. B **4**, 3321 (1971).
[32] V.N. Antonov, A.I. Baglyuk, A.Ya. Perlov, V.V. Nemoshkalenko, O.K. Andersen, and O. Jepsen, Low Temp. Phys. **19**, 689 (1993).
[33] G.A. Bolotin, M.M. Kirillova, and V.M. Maevskij, Phys. Met. Metallogr. **27**, 224 (1969).
[34] J.H. Weaver, E. Colavita, D.W. Lynch, and R. Rosei, Phys. Rev. B **19**, 3850 (1979).
[35] D.G. Laurent, J. Callaway, and C.S. Wang, Phys. Rev. B **20**, 1134 (1979).
[36] J.H. Sexton, D.W. Lynch, R.L. Benbow, and N.V. Smith, Phys. Rev. B **37**, 2879 (1988).
[37] Y.A. Uspenski and S.V. Khalilov, Zh. Eksp. Teor. Fiz. **95**, 1022 (1989) [Sov. Phys. JETP **68**, 588 (1989)].
[38] P.M. Oppeneer, T. Maurer, J. Stricht, and J. Kübler, Phys. Rev. B **45**, 10 924 (1992).
[39] N. Mainkar, D.A. Browne, and J. Callaway, Phys. Rev. B **53**, 3692 (1996).
[40] G.S. Krinchik and V.S. Gushchin, Zh. Eksp. Teor. Fiz. **56**, 1833 (1969) [Sov. Phys. JETP **29**, 984 (1969)].
[41] J.L. Menéndez, G. Armelles, A. Cebollada, D. Weller, and A. Delin, Phys. Rev. B **62**, 10 498 (2000).
[42] G.S. Krinchik, *Physics of Magnetic Phenomena* (MGU, Moscow, 1976).
[43] G.Y. Guo and H. Ebert, J. Magn. Magn. Mater. **156**, 173 (1996).
[44] G.Y. Guo and H. Ebert, Phys. Rev. B **51**, 12 633 (1995).